8973-26-F

THE MEASUREMENT OF WATER DEPTH BY REMOTE SENSING TECHNIQUES

F. C. POLCYN
W. L. BROWN
I. J. SATTINGER

October 1970

INFRARED AND OPTICS LABORATORY
Willow Run Laboratories
INSTITUTE OF SCIENCE AND TECHNOLOGY

Prepared for the Spacecraft Oceanography Project,
U. S. Naval Oceanographic Office, Washington, D. C.

Contract N62306-67-C-0243

48

8973-26-F

THE MEASUREMENT OF WATER DEPTH BY REMOTE SENSING TECHNIQUES

F. C. POLCYN
W. L. BROWN
I. J. SATTINGER

October 1970

Infrared and Optics Laboratory
Willow Run Laboratories
THE INSTITUTE OF SCIENCE AND TECHNOLOGY
THE UNIVERSITY OF MICHIGAN
Ann Arbor, Michigan

FOREWORD

The work reported herein has been sponsored by the Spacecraft Oceanography Project, NAVOCEANO, Washington, D. C. and carried out by the Willow Run Laboratories, a unit of the The University of Michigan's Institute of Science and Technology in Ann Arbor, under the direction of Marvin R. Holter, Head, Infrared and Optics Laboratory. Mr. John Sherman III is manager of the SPOC Project and provided technical monitoring of the investigation.

This document is the second annual report prepared under contract No. N62306-67-C-0243. These studies are to be continued under NASA sponsorship under contract NAS-9-9784. The Willow Run Laboratories' number for this report is 8973-26-F.

This report is one of a series in a program of remote sensing research initiated by M. R. Holter. A list of related reports in this program follows on succeeding pages.

RELATED REPORTS

TARGET SIGNATURE STUDY, INTERIM REPORT, VOLUME V: CATALOG OF SPECTRAL REFLECTANCE DATA, R. R. Legault, R. S. Gould, and T. Limperis, Report No. 5698-22-T(V), Institute of Science and Technology, The University of Michigan, Ann Arbor, October 1964 (Published as part of Data Compilation, AD 489 968, see p. vi).

THE INVESTIGATION OF A METHOD FOR REMOTE DETECTION AND ANALYSIS OF LIFE ON A PLANET, M. R. Holter, D. S. Lowe, and J. R. Shay, Report No. 6590-1-P, Institute of Science and Technology, The University of Michigan, Ann Arbor, November 1964.

THE INVESTIGATION OF A METHOD FOR REMOTE DETECTION OF LIFE ON A PLANET, L. D. Miller, Report No. 6590-4-F, Willow Run Laboratories of the Institute of Science and Technology, The University of Michigan, Ann Arbor, Michigan, November 1965.

UNUSUAL RECONNAISSANCE CONCEPTS INTERIM REPORT, VOLUME II: SOURCES OF EXPERIMENTAL ERRORS IN SPECTROPHOTOMETRIC MEASUREMENTS, Dianne Goerge and T. Limperis, Report No. 5698-33-(II), AFAL-TR-65-331, Willow Run Laboratories of the Institute of Science and Technology, The University of Michigan, Ann Arbor, January 1966, AD 481 796.

UNUSUAL RECONNAISSANCE CONCEPTS INTERIM REPORT, VOLUME III: A BIBLIOGRAPHY OF RECENT CONTRIBUTIONS ON ELECTROMAGNETIC AND ACOUSTIC SCATTERING, J. Ulrich, Report No. 5698-33-P-(III), AFAL-TR-65-331, Willow Run Laboratories of the Institute of Science and Technology, The University of Michigan, Ann Arbor, January 1966, AD 481 817.

TARGET SIGNATURE ANALYSIS CENTER: DATA COMPILATION, D. G. Earing and J. A. Smith, Report No. 7850-2-B, Willow Run Laboratories of the Institute of Science and Technology, The University of Michigan, Ann Arbor, July 1966, AD 489 968.

DISPERSIVE MULTISPECTRAL SCANNING: A FEASIBILITY STUDY, FINAL REPORT, J. Braithwaite, Report No. 7610-5-F, Willow Run Laboratories of the Institute of Science and Technology, The University of Michigan, Ann Arbor, September 1966.

AN INVESTIGATIVE STUDY OF A SPECTRUM-MATCHING IMAGING SYSTEM, FINAL REPORT, D. S. Lowe, J. Braithwaite, and V. L. Larrowe, Report No. 8201-1-F, Willow Run Laboratories of the Institute of Science and Technology, The University of Michigan, Ann Arbor, October 1966.

DATA SIGNATURE ANALYSIS CENTER: DATA COMPILATION (SUPPLEMENT), D. Earing, Report No. 7850-9-B, Willow Run Laboratories of the Institute of Science and Technology, The University of Michigan, Ann Arbor, January 1967, AD 379 650.

OPTICAL SENSING OF MOISTURE CONTENT IN FINE FOREST FUELS, FINAL REPORT, C. E. Olson, Jr., Report No. 8036-1-F, Willow Run Laboratories of the Institute of Science and Technology, The University of Michigan, Ann Arbor, May 1967.

TARGET SIGNATURE ANALYSIS CENTER: DATA COMPILATION (SECOND SUPPLEMENT), D. Earing, Report No. 8492-5-B, Willow Run Laboratories of the Institute of Science and Technology, The University of Michigan, Ann Arbor, July 1967, AD 819 712.

WILLOW RUN LABORATORIES

TARGET SIGNATURE ANALYSIS CENTER: DATA COMPILATION (FIFTH SUPPLEMENT), D. Earing, Report No. 8492-15-B, Willow Run Laboratories of the Institute of Science and Technology, The University of Michigan, Ann Arbor, August 1968.

CALIBRATION OF AN AIRBORNE MULTISPECTRAL OPTICAL SENSOR, L. M. Larsen and P. G. Hasell, Jr., Report No. 6400-137-T, Willow Run Laboratories of the Institute of Science and Technology, The University of Michigan, Ann Arbor, September 1968.

TARGET SIGNATURE ANALYSIS CENTER: DATA COMPILATION (SIXTH SUPPLEMENT), D. Earing, Report No. 8492-26-B, Willow Run Laboratories of the Institute of Science and Technology, The University of Michigan, Ann Arbor, October 1968.

INVESTIGATIONS OF SPECTRUM-MATCHING TECHNIQUES FOR REMOTE SENSING IN AGRICULTURE, Final Report, Report No. 1674-10-F, Willow Run Laboratories of the Institute of Science and Technology, The University of Michigan, Ann Arbor, December 1968.

EFFECTS OF ATMOSPHERIC PATH ON AIRBORNE MULTISPECTRAL SENSORS R. Horvath, J. G. Braithwaite, F. C. Polcyn, Report No. 1674-5-T, Willow Run Laboratories of the Institute of Science and Technology, The University of Michigan, Ann Arbor, December 1968.

APPLICATIONS OF MULTISPECTRAL REMOTE SENSING TECHNIQUES TO HYDROBIOLOGICAL INVESTIGATIONS IN EVERGLADES NATIONAL PARK, A. L. Higher, N. S. Thomson, F. J. Thomson, M. C. Kolipinski, Technical Report 2528-5-T, January 1970, (Joint Report of The University of Michigan and the U. S. Department of the Interior).

TARGET TEMPERATURE MODELING, D. Bornemeier, R. Bennett, R. Horvath, Final Technical Report RADC-TR-69-404, Willow Run Laboratories, Institute of Science and Technology, The University of Michigan, Ann Arbor, December 1969.

HOW MULTISPECTRAL SENSING CAN HELP THE ECOLOGIST, F. C. Polcyn, N. A. Spansail, W. A. Malila, Remote Sensing in Ecology, University of Georgia Press, 1969.

INVESTIGATION OF MULTISPECTRAL DISCRIMINATION TECHNIQUES, R. F. Nalepka, Final Technical Report 2264-12-F, Willow Run Laboratories, Institute of Science and Technology, The University of Michigan, Ann Arbor, January 1970.

USE OF MULTISPECTRAL RECOGNITION TECHNIQUES FOR CONDUCTING RAPID, WIDE AREA WHEAT SURVEYS, R. E. Marshall and N. S. Thomson, Proceedings of the Sixth Symposium on Remote Sensing of the Environment, The University of Michigan, Ann Arbor, October 1969.

A SPECTRAL DISCRIMINATION TECHNIQUE FOR AGRICULTURAL APPLICATIONS, D. G. Earing and I. W. Ginsberg, Proceedings of the Sixth Symposium on Remote Sensing of the Environment, The University of Michigan, Ann Arbor, October 1969.

APPLICATION OF MULTISPECTRAL DATA AND PROCESSING TECHNIQUES TO THE DISCRIMINATION OF SINKHOLE ACTIVITY IN FLORIDA, A. E. Coker, U. S. Geological Survey, Tampa, Florida, and R. E. Marshall and N. S. Thomson, The University of Michigan, Ann Arbor, Proceedings of the Sixth Symposium on Remote Sensing of the Environment, The University of Michigan, Ann Arbor, October 1969.

WATER DEPTH DETERMINATIONS USING REMOTE SENSING TECHNIQUES, F. C. Polcyn and I. J. Sattinger, Proceedings of the Sixth Symposium on Remote Sensing of the Environment, The University of Michigan, Ann Arbor, October 1969.

REFLECTANCE AND EMITTANCE FROM BROADLEAVED TREES DURING PERIOD OF PHYSIOLOGIC STRESS, C. E. Olson, Jr., W. G. Rohde, and J. M. Ward, Proceedings of the Sixth Symposium on Remote Sensing of the Environment, The University of Michigan, Ann Arbor, October 1969.

PREPROCESSING TRANSFORMATIONS AND THEIR EFFECTS ON MULTISPECTRAL RECOGNITION, F. Kriegler, W. Malila, R. Nalepka and W. Richardson, Proceedings of the Sixth Symposium on Remote Sensing of the Environment, The University of Michigan, Ann Arbor, October 1969.

MEASUREMENTS PROGRAM FOR OIL SLICK CHARACTERISTICS, FINAL REPORT, R. Horvath, W. L. Morgan, R. Spellicy, Report No. 2766-7-F, Willow Run Laboratories of the Institute of Science and Technology, The University of Michigan, Ann Arbor, February 1970.

ATMOSPHERIC EFFECTS ON MULTISPECTRAL SENSING OF SEA SURFACE TEMPERATURE FROM SPACE FOR CLEAR ATMOSPHERES, QUARTERLY REPORT, D. Anding, R. Kauth, Report No. 2676-2-P, Willow Run Laboratories of the Institute of Science and Technology, The University of Michigan, Ann Arbor, June 1970.

MULTISPECTRAL REMOTE SENSING OF URBAN FEATURES, J. E. Colwell, Report No. 2772-6-F, Willow Run Laboratories, Institute of Science and Technology, The University of Michigan, Ann Arbor, March, 1970.

AN INVESTIGATION OF GRASSLAND RESOURCES USING MULTISPECTRAL PROCESSING AND ANALYSIS TECHNIQUES, T. W. Wagner and J. E. Colwell, Report No. 34795-1-F, Willow Run Laboratories, Institute of Science and Technology, The University of Michigan, Ann Arbor, in preparation.

ABSTRACT

This study demonstrates successful remote determination of shallow water depth by measuring wave refraction changes and using the Fourier transform plane for wavelength measurements with data obtained at a Lake Michigan test site. The study shows that the technique is suitable for use from spacecraft altitudes, provided that water waves of suitable length occur in the region of interest.

A second demonstration of remote measurement of water depth was performed using data collected at Caesar Creek in the Florida Keys. For the first time, a newly developed multispectral technique, based on a ratio of reflected radiation in at least two spectral bands in the visible region of the spectrum, was used to determine water depth. Data were collected with The University of Michigan's multispectral scanner and recorded on magnetic tape. By digitizing the data and correcting for surface reflections, a depth chart can be generated from computer output.

An analysis of laser systems suitable for water depth determinations is also provided. It is anticipated that the use of laser depth measurements with the multispectral computer printout will provide best accuracy.

CONTENTS

FIGURES

TABLES

THE MEASUREMENT OF WATER DEPTH BY REMOTE SENSING TECHNIQUES

1 INTRODUCTION

In a previous study (Ref.1), four variables were identified on which a remote sensor might operate in order to measure depth or deduce the location of shallower water. The four variables included temperature changes, color changes, wave refraction, and time differences for laser pulse reflections. As in all detection problems, a classification of a particular depth is more reliable if it depends on a convergence of evidence from several sensors.

Since it was found that temperature changes were useful for locating shallow water out not for measuring depth, this report concentrates on the use of the latter three variables for depth measurements performed in three ways.

(1) By measuring wave refraction effects in the Fourier transform domain produced by an optical processor, with an aerial photograph used as the input transparency. This technique, discussed in Section 2, lends itself to use from any altitude, including those of earth satellites, and is independent of the light transmission characteristics of water.

(2) By measuring at different spectral intervals the relative intensities of light reflected by the ocean or lake bottom and correcting for surface reflection and scattering, using a multispectral scanner such as that developed by The University of Michigan. The first depth measurements made by these techniques are reported in Section 3.

(3) By measuring the time difference of laser pulses reflected from the water surface and from the bottom. This technique (see Section 4) provides an independent measure of the water depth at sample locations.

It is the ultimate goal of this project to combine the latter two techniques: laser depth measurement taken along transects, with two-dimensional depth contours produced with the multispectral digital-processing technique described in this report. The result will be a system of making rapid surveys of near-shore environments or other regions about which knowledge of water depth is needed to reduce hazards to ship navigation, to aid marine engineering projects, to study shore erosion, to permit quick assessment of storm-induced changes, and to aid in investigation of lake level and estuarine problems.

Although this is the second annual report to be prepared under Contract N62306-67-C-0243, the study is not yet complete; it will be continued under NASA sponsorship (Contract NAS-9-9784).

2
WAVE ANALYSIS TECHNIQUES

Optical data-processing techniques can be adapted to measure water depth by analyzing the characteristics of water waves as recorded by aerial or space photography. It is known that shoal areas and beaches influence both the wavelength and the direction of waves passing over them. The forward velocity of a wave train decreases appreciably when the waves pass over an area in which the water depth is less than about half the wavelength. In addition to noting the change in typical wavelength directly on the original photograph, the change could be observed in other ways. An indirect effect of shoal areas and beaches is to increase the wave height, producing breakers; thus, breakers are another indication of shallow water. Another effect is to cause refraction of the wave, resulting in a change in azimuth of the wavefront and a corresponding change in the direction of wave advance.

The change in wavelength and in wavefront orientation can be observed by subjecting the original images to certain optical data-processing methods (Ref. 2). When a portion of the original image is illuminated by coherent light, such as that produced by a laser, and the transmitted light is focused by the use of a spherical lens, the resulting presentation on a screen at the focal point of the lens shows, in a polar coordinate frame, the distribution of both wavelength and wavefront orientation contained in the illuminated portion of the original image. It should, therefore, be possible to analyze aerial photography of sea surfaces both to detect shoal areas initially and to measure water depth in these areas.

2.1. METHODS OF DEPTH MEASUREMENT USING WAVE ANALYSIS

Several computational procedures can be used in estimating water depth from measurements of aerial photography. The analytical basis for these various procedures is discussed in this section, and experimental studies of individual procedures are presented in Section 2.3.

First order theory of wave swells describes a train of waves advancing through deep water as having a velocity related to its wavelength and wave period as in the following equations:

$$L_o = 5.12\ T^2 \tag{1}$$

$$C_o = \frac{L_o}{T} = 5.12\ T \tag{2}$$

where L_o = deep-water wavelength (ft)
C_o = deep-water wave velocity (fps)
T = wave period (sec)

As waves approach shallow water of depth, d, the velocity of wave advance, C, and the wavelength, L, decrease appreciably for values of d/L_o less than about 0.5.

This change in wave velocity is related to the fact that in shallow water the motion of individual particles of water is modified. In deep water, the orbit of each particle of water is circular in shape, with the radius of the circle decreasing rapidly with depth. In shallow water, the closeness of the bottom modifies the orbit to elliptical form, which has an effect on the forward velocity.

Since the period of a given wave train remains constant at all points along its path, a changing forward velocity changes the wavelength. It is therefore possible to measure depth from aerial photography by first measuring wave separation and directions of waves both in the shoal areas and in deep areas (deep is defined relative to the wavelength of the incoming waves). The wavelength in deep water (L_0) and the wavelength in shallow water (L) can be measured in a single aerial photograph. The measured ratio of wavelengths, L/L_0, is functionally related to the ratio d/L_0, so that depth, d, can be determined (Ref. 3). The optical data-processing methods discussed in the following sections provide an effective means of measuring L and L_0.

When waves approach a beach at an angle, changes in the velocity of wave advance lead to changes in the wave orientation caused by refractive effects. The change in direction from deep to shallow water can also be accurately measured by optical data-processing methods. This approach is applicable, for example, for straight beaches with parallel contours. The direction of the incoming wave and the direction of the wave at the point of depth measurement are observed. These two measurements determine the ratio of depth, d, to deep water wavelength, L_0. If L_0 is also measured, the depth can be determined. However, the measurement of changes in wave direction to determine depth presents complications. Where the bottom contour cannot be assumed as straight, the method must be modified by preparing a refraction diagram of the area of interest, extending into the ocean to points where the depth is equal to at least half the observed wavelength. As a means of detecting shoal areas, as distinguished from measuring them, the measurement of wave direction changes can be effective, provided the orientation of incoming waves is sufficiently regular to avoid masking the effect of the shoals.

Other approaches to depth measurement can be used if successive photographs at short intervals can be provided. Under these conditions, it becomes possible to measure not only wavelength and wave direction, but also wave velocity and wave period. If two pictures are taken at a known interval of time, the wave velocity in deep water, C_0, and in the test area, C, can be determined. (To make accurate measurement of wave advance over a short time interval, a fixed reference point must be apparent in each photograph.) The wave velocity can be computed, by noting the change in wave position, as the ratio of distance traveled by the wave to the time interval between observations. The ratio C/C_0 derived from these pictures is equal to the ratio L/L_0 and can thus be used to determine d/L_0. Wavelength can be measured directly from the photograph.

Another alternative would be to measure L and C in the shoal area only. Wave period, T, can be computed as the ratio of wavelength to wave velocity, L/C. The wave period remains constant as the wave travels from deep to shallow water; hence, the measurement of T provides a means of computing L_o or C_o by the use of Eqs. (1) or (2). This method thus requires measurements only in the test area and eliminates the need for measurements in deep water. Its accuracy depends on the regularity of the wave patterns present at the time of measurement and on the resolution of the photography.

2.2. APPLICATION OF FOURIER TRANSFORM PROCESSING

Optical data processing has been performed on a number of aerial photographs covering both open sea and shoal areas, such as beaches and reefs. A generally valid relationship has been found between the wave characteristics as measured from the aerial photograph and the wavelength and orientation characteristics recorded by the optical processor. If a swell or local wave pattern with a clearly defined orientation and predominant wavelength content is apparent on the aerial photograph, the Fourier transform pattern produced by the optical processor will tend to show this dominant wave pattern as a circular dot of finite size at the appropriate wavelength and angle. Distance of the dot from the center of the pattern is inversely proportional to wavelength. The finite size of the dot indicates a scatter, in both wavelength and direction in the original imagery, to be expected in wave patterns, even under favorable conditions. The irregularity of the fundamental pattern and the existence of local chop will tend to introduce both lower and higher frequency components into the Fourier transform. In many cases, therefore, the idealized dot pattern expected for a single sinusoidal wave component becomes elongated to include a considerable variation of wavelength components. The angular spread is less affected, so that, in many examples, wave direction may be determined more accurately than the wavelength itself.

The interrelation of sun elevation, view angle, and wave spectrum appears to have some effect on the transform representation of a particular area. The wave pattern is most visible at the edges of the sun-glitter pattern, and may be nearly invisible at the center of the pattern or far outside the pattern. Sun glitter seems to emphasize those wave crests which are tangent to the sun-glitter circle. If further study confirms this effect, it may be used to advantage in eliminating the confusion resulting from the existence of several wave patterns.

The conclusions reached so far are that the two-dimensional Fourier transform gives a useful indication of dominant wavelength and direction. To obtain accurate measurements, (1) the wave pattern must be a fairly regular one and not a confused combination of several different wave trains; and (2) the proper exposure and sun-glitter pattern must be used. It is believed that additional investigation will improve the definition of the best conditions of use and develop refinements in technique which would further increase the accuracy of determining wavelength and wave direction.

2.3. EXAMPLES OF OPTICAL DATA-PROCESSING TECHNIQUES FOR MEASURING DEPTH

As a quantitative example of the use of several wave analysis techniques for measuring water depth, an aerial photograph taken near the exit of the Grand River into Lake Michigan near Grand Haven was used. (See Figs. 1 and 2.) The objective of the task was to determine the depth of water in two areas, A and B. Area A is a rectangular area, 500 × 1300 ft, parallel to the shoreline, with its near edge about 270 ft offshore. Area B is a rectangular area of the same dimensions and orientation but with its near edge about 1600 ft offshore. To determine deep-water wavelength, L_o, wave measurements were also made over Area C. The depth of water in Area C, approximately 40-45 ft, did not have an appreciable effect on the length or direction of the waves passing over it at the time the photograph was taken.

Two methods of calculation were used, one based on the difference in wavelength in Area A and Area C, and the other based on the change in direction of the waves in these two areas. Measurements of wavelength and wave direction were each made in more than one way to compare various techniques available.

We will consider first the determination of water depth by wavelength measurement. Measurements of wavelength were scaled directly from the aerial photograph and were also obtained from a Fourier transform made by optical processing (Fig. 3). The results of these measurements are shown in Table 1. Using the data taken from the Fourier transform measure-

FIGURE 1. LAKE MICHIGAN SHORELINE AT GRAND HAVEN

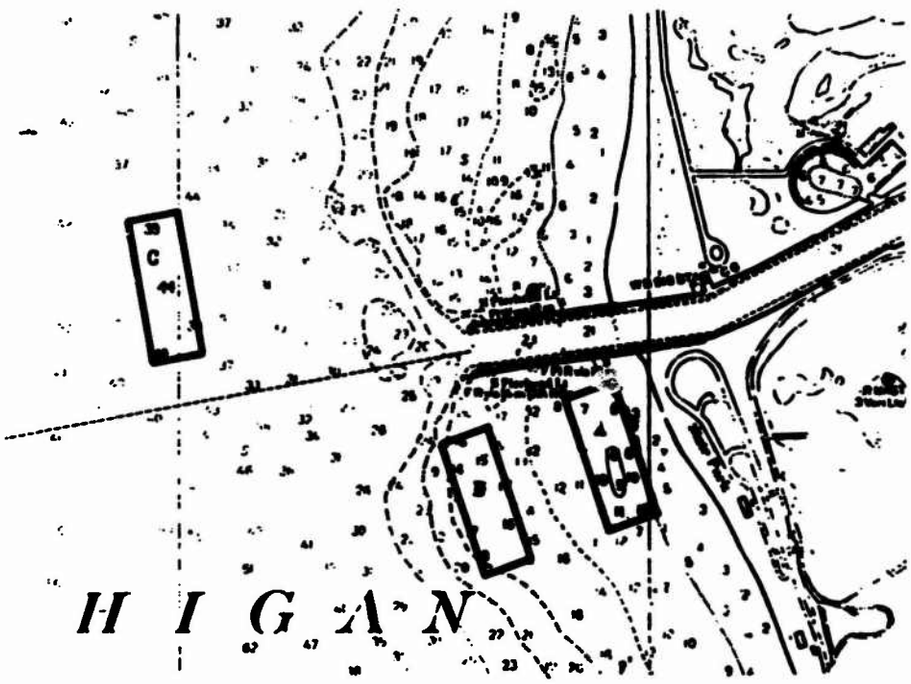

FIGURE 2. LAKE SURVEY CHART —GRAND HAVEN, MICHIGAN

TABLE 1. WAVELENGTHS DETERMINED BY TWO METHODS

Method	Area A	Area B	Area C
Direct measurement of aerial photograph	53	82	92
Fourier transform	56.5	70	80

ments, the depth of Area A was found to be 7.9 ft. Inspection of Lake Survey Chart Number 765 of the Michigan coastline at Grand Haven indicates that the depth of Area A ranges from 6 to 10 ft. Fourier transform measurements were also used to compute the depth of Area B. The computed depth was 15 ft; depths determined from the chart ranged from 14 to 18 ft.

Water depth in Area A was also computed by comparing the angle of the incoming wave in Area A with that of Area C, where the wave orientation was presumably still outside the influence of the shore. Angle measurements were made by reference to both the original photograph and the Fourier transform.

Both methods gave values of 60^{o} for Area C and 35^{o} for Area A, measured with respect to the shoreline. Using these values, the value of d/L_o for Area A can be obtained by using data

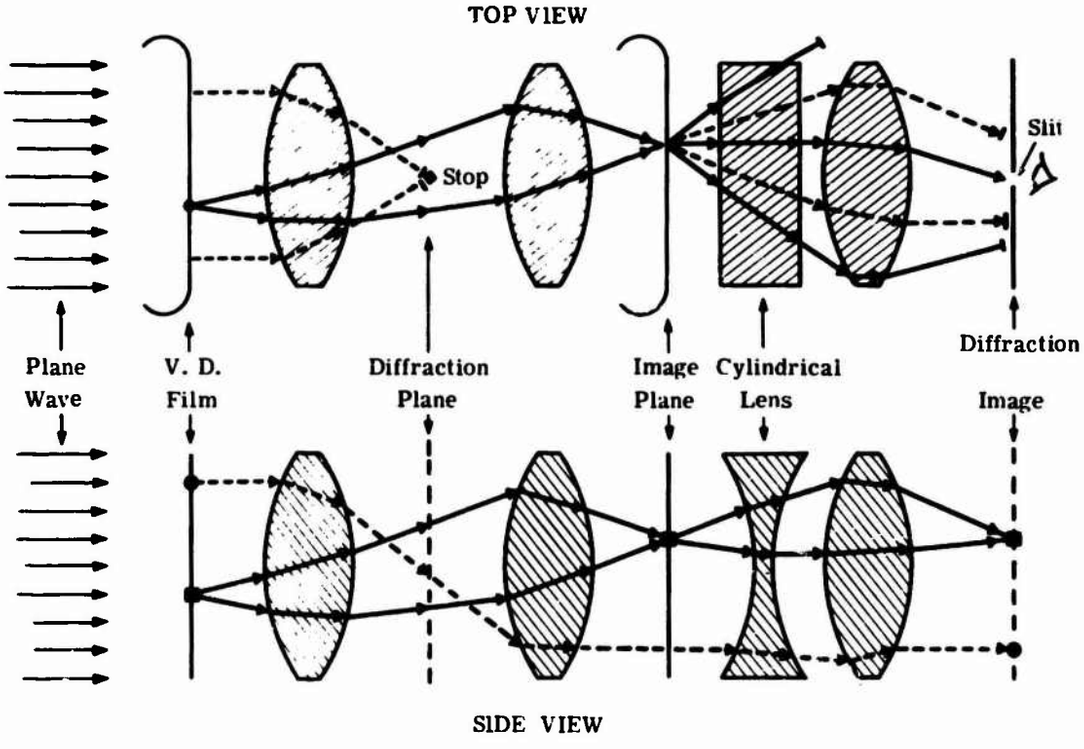

FIGURE 3. DIFFRACTIVE OPTICAL SYSTEM

such as that published in Ref. [4]. The value obtained for d/L_o was found to be 0.086, and using the wavelength of 80 ft from Table 1, the water depth in Area A is computed as 6.9 ft, which checks closely with the value determined by wavelength measurements. For Area B, the angle of approach was 45°, giving an estimated depth of 12.0 ft. This is appreciably less than the chart value of 14-18 ft.

2.4. EFFECT OF ALTITUDE AND CLOUD COVER

The data from Mission 72, Lake Michigan, together with data from Mission 79, Gulf of Mexico, and samples of satellite photography provided an initial data base to study the effect of increasing altitude and cloud cover on the generation of interpretable optical transforms and on the measurement of wavelength. One of the advantages in using the optical transform is that at smaller photographic scales, the dot separation from the center in the transform increases and less confusion results in the bright central portion of the transform pattern. Figure 4, taken from an area near Cayo Arenas in the Gulf of Mexico, illustrates this effect. The area is in open deep water away from the diffraction effects caused by the island or refraction effects due to submerged shoals. The photography was taken at an altitude of 22,000 ft with a 6-in. focal length lens. Note the clean separation of the dot pattern for the fundamental wave component

FIGURE 4. CAYO ARENAS—(GULF OF MEXICO)

of the sea surface (see Figure 5). Figure 6 shows the transforms taken nearer the island at three different locations; the azimuthal changes in wave direction due to the diffraction of waves around the island are shown clearly in the transform domain when compared to the transform in Fig. 5.

The wavelengths measured in the sun-glitter region in Fig. 6 were in the 100-ft range but no depth measurements were made in the area since depths of 50 ft or less were not present. The required ratio of depth to wavelength of less than one-half implies that a determination of depth in a given area will depend on the existence of a particular set of conditions at the time the data is taken. Since these conditions may not always exist, a technique is needed to analyze rapidly many photographs in which routine data has been taken for a variety of other purposes. It is expected that scanning the transform plane for the dot separation will be a quicker and simpler method than scanning the original photograph.

Additional tests were also made of the effects of cloud patterns in portions of the photograph. Figure 7 shows a comparison of two transforms taken from sections of the photograph with and without cloud obscuration. The fundamental wavelength component was observed in both cases. The large cloud pattern generally transforms into the lower spatial frequencies located near the center. The presence of scattered clouds does effect the overall exposure

(a) Aerial Photograph

(b) Fourier Transform

FIGURE 5. WAVES IN OPEN WATER

during the construction of the optical transform, indicating that an increase in exposure time may be necessary in some cases.

2.5. SPACE PHOTOGRAPHY

Frame AS7-4-1607 taken during the Apollo 7 flight distinctly shows a widespread, long wavelength swell moving in the direction of the Schouten Islands near New Guinea. The swell has an extremely regular pattern, consisting of wave crests many miles in length, essentially straight, with little or no apparent variation in wavelength. This type of wave pattern would have been caused by a recent storm at a considerable distance; the dispersive characteristic of water waves has separated the wavelength components in the storm area, so that only a single wavelength is present in the picture.

Optical data processing was applied to one section of this picture in which the wave pattern was most distinct (Fig. 8a). The resulting transform shows a very definite wave component ranging from 1040 to 1220 ft and an orientation angle ranging from 40 to 50°. Corresponding to the figures derived from the transform, measurements made from the original image indicated a typical wavelength of 1100-1200 ft and an orientation angle of 45°. An analysis of this frame has also been performed by Noble (Ref. 5).

(a) Aerial Photograph (West of Cayo Arenas)

(b) Fourier Transform

FIGURE 6. DIFFRACTION OF WATER WAVES

The swell can be seen reaching the large island shown in the picture, but because the sun-glitter pattern in the vicinity of the island provides only a low contrast in the wave image, it is difficult to obtain a transform pattern in this region. Measurements taken from the original image indicate that the wavelength becomes shorter in the vicinity of the island, but the wave direction does not appear to change appreciably. The long wavelengths composing the swell would be sensitive to relatively great bottom depths and are thus most likely to provide useful information concerning shallow water. It would be highly desirable to obtain imagery of long swells approaching land at shorter intervals between frames so that every part of the water surface of interest is in the favorable part of the sun-glitter pattern on at least one exposure.

Frame AS6-2-918 of Apollo 6 imagery shows an extensive wave system covering large areas of open ocean. The transform taken over a part of the frame (see Fig. 8b) representing a rectangle many miles on a side shows a wave system consisting predominantly of wavelengths ranging from 850 to 1050 ft over an angular range of 20^{o}. Typical measurements from the original image show a wavelength of 1020 ft at an angle in the exact center of the angular range If wave patterns with the easily identifiable limits shown in this example were available in the

(a) Aerial Photograph

(b) Fourier Transform

FIGURE 7. CLOUDS AND CLOUD SHADOWS

neighborhood of islands of shallow areas, it should be possible to detect and measure shallow water with fair accuracy.

Measurements were made from Fourier transforms taken of Apollo frame AS7-4-1607 and AS6-2-918 in order to determine the precision of wavelength and angle measurements produced by optical data-processing techniques, using manual data reduction by scale and protractor. Frame AS7-4-1607 is distinguished by the fact that the wave system is very regular as to both wavelength and wave orientation. The results of optical data processing on this frame indicate that wavelength measurements can be obtained with a precision of 2 or 3% and angle measurements with a precision of 2 or 3°. Assuming that this precision could be obtained in measuring both L and L_o, it is possible to estimate the accuracy of computing depth for a known value of d/L_o. If d/L_o is equal to 0.100, for example, the depth could be estimated within about ±10%. (In the Lake Michigan example previously presented, Area A had a d/L_o of about 0.100.)

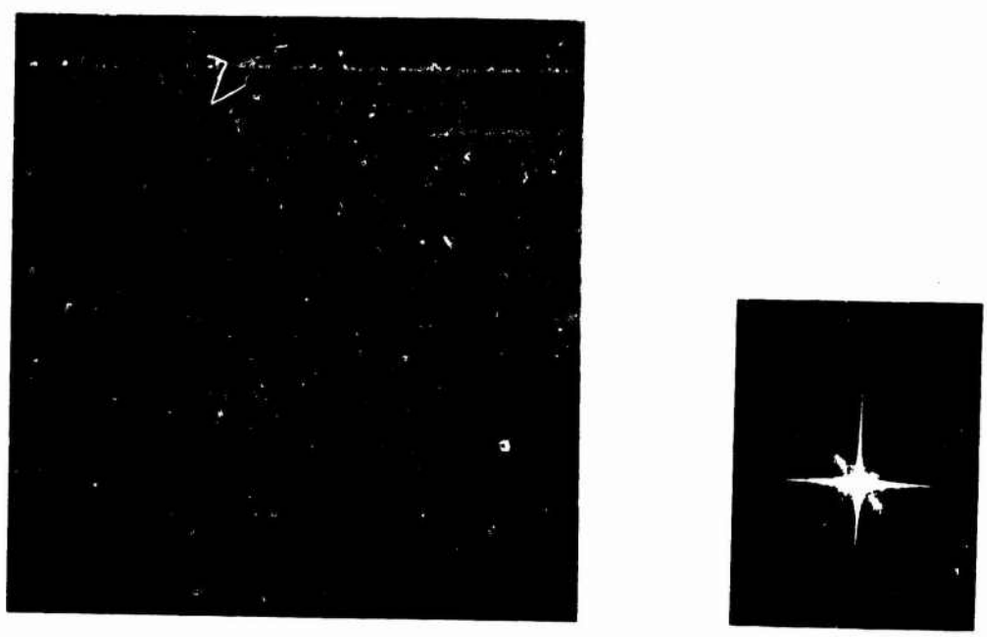

(a) Apollo 7 Frame AS7-4-1607

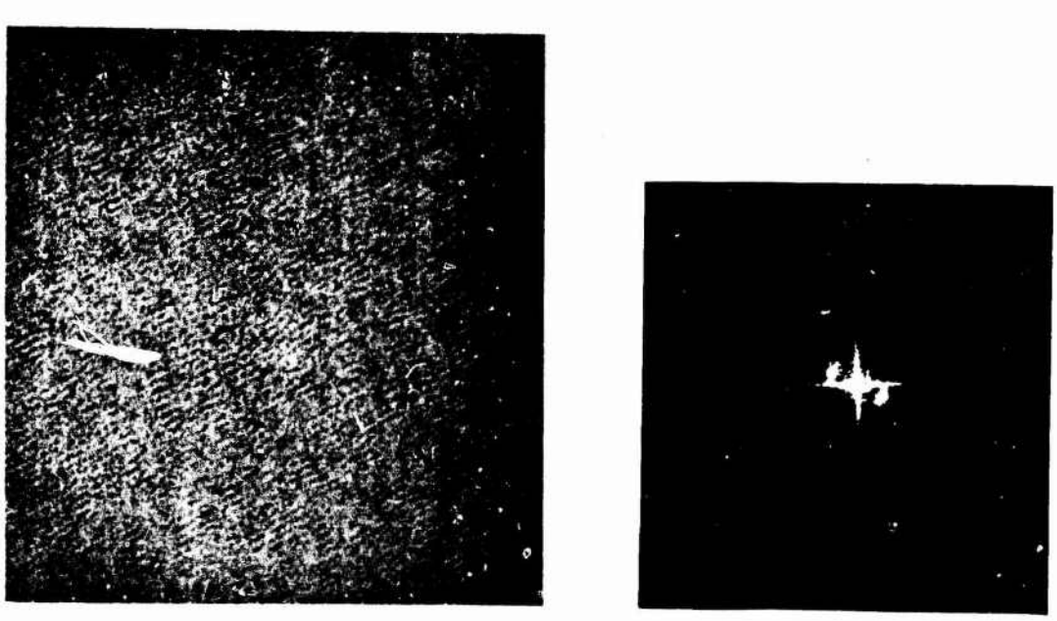

(b) Apollo 6 Frame AS6-2-918

FIGURE 8. OPTICAL DATA PROCESSING

2.6. ALTERNATIVE METHODS OF OPTICAL DATA PROCESSING

2.6.1. TWO-DIMENSIONAL CROSS-CORRELATION PROCESSING

Other optical data-processing approaches to the problem of detecting and measuring shoal areas were investigated during this project to determine their potential advantages compared to the use of two-dimensional Fourier transform approach. For example, a two-dimensional cross correlation of the sea-surface image would contain information similar to that contained in the Fourier transform, but would have the advantage that the scale of output presentation is not tied as rigidly to the scale of the original image transparency placed in the optical data-processing system. It is possible, therefore, that relatively small sea-surface areas at relatively large scales could be used for processing. This would improve the spatial resolution with which wave data could be processed, although it would not reduce the scatter in the wave data.

As a typical example of results obtainable by this method, a cross-correlation display was made of a portion of Frame 8402 taken of Lake Michigan beach which contains a linear wave pattern approaching the beach. (See Fig. 9 for the input transparency made from the photograph.) This wave pattern is oriented at an angle of approximately 20°. The output produced by taking the cross-correlation of Fig. 9 is a broad band, oriented at approximately the same angle, representing the high correlation of the light-reflectance pattern along the wave crest. This broad band is bound on either side by two parallel dark bands representing the difference in reflectance between the wave crest and the adjacent wave troughs. The separation between the centers of the dark bands, produced at a scale of 7.4 times the scale of the original image, corresponds to the dominant wavelength in the image. Thus, the cross-correlation diagram can show the orientation and wavelength of a well defined wave pattern. The diagram can be adjusted for use with a broad range of photographic scale factors and can be restricted to coverage of small sea-surface areas. However, it seems to be more difficult to set up and work with, and more difficult to interpret than the Fourier transform, particularly if several wave trains are present at the same time. Although its use should not be ruled out on the basis of the brief investigation made so far, the present study has been concentrated on other methods.

2.6.2. SECTIONAL AUTOCORRELATION DIAGRAMS

Figure 10 is an example of a sectional autocorrelation diagram of a small area taken from Frame 1037 of the Lake Michigan shoreline. In this type of data analysis, the variable density pattern of a linear strip of the original photograph orthogonal to the wave crests is transformed into a corresponding linear strip on the autocorrelation diagram, the brightness of which corresponds to the autocorrelation of the signal on the original linear strip. (See Ref. 4.) The autocorrelation diagram along a vertical strip at any given value of x thus corresponds to the wave pattern along a vertical strip of the original image at a proportional distance along its x axis;

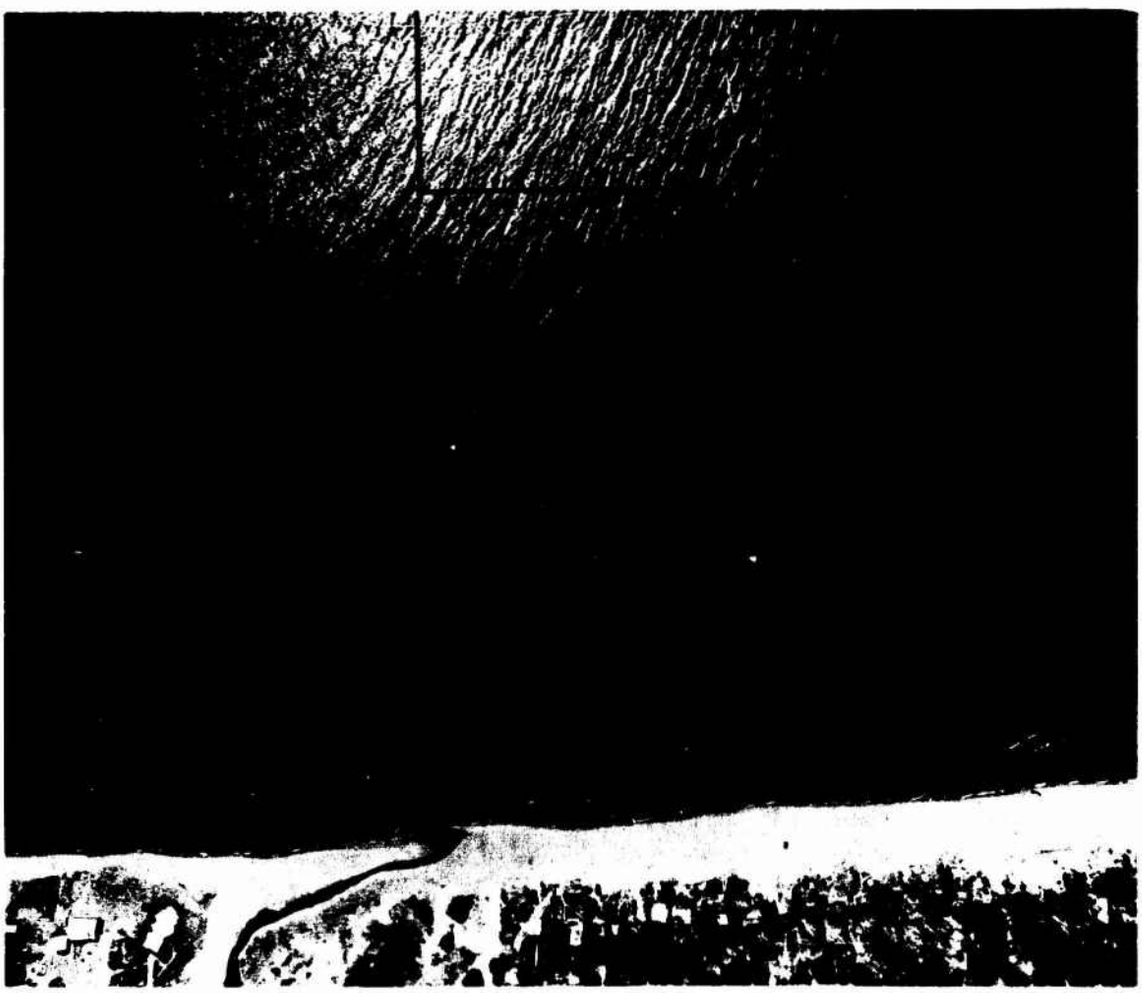

FIGURE 9. INPUT TRANSPARENCY FOR CROSS-CORRELATION OPERATION ON FRAME 8402 —LAKE MICHIGAN BEACH

however, the scales are not necessarily equal on the two diagrams. The bright band near the center of the diagram corresponds to the peak value of the autocorrelation function for $\tau = 0$. In both directions from this bright band, the brightness varies with distance from the center, i.e., increasing magnitudes of τ, both positive and negative as distance from the center increases. The periodic character of the autocorrelation pattern indicates the presence of periodic variations in the original image, and the predominant wavelength in the original can be measured from the autocorrelation diagram, using a fixed scale factor determined by the optical setup. It should be noted that the sectional autocorrelation detects wavelength components only in one direction; components at right angles to this direction are not recorded.

The sectional autocorrelogram is useful in bringing out the predominant wavelength present in the original image. Where the original image has a regular pattern of waves, the perio-

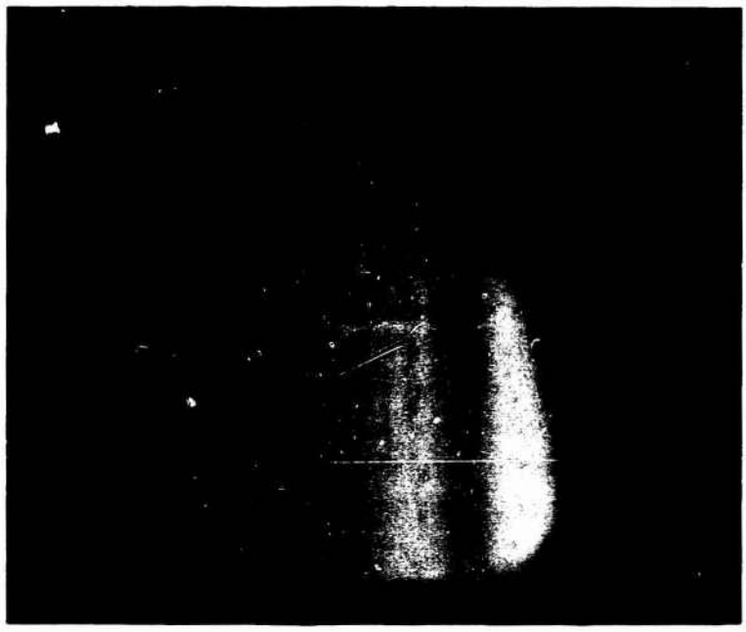

FIGURE 10. SECTIONAL AUTOCORRELATION OF FRAME 1037

dicity present in the autocorrelation diagram is apparent for 5 or 6 cycles and the wavelength on this diagram is easy to measure. However, the extent of the periodicity and its wavelength vary substantially depending on the position of the strip along the x axis of the diagram, indicating the variability inherent in the original image. Nevertheless, this form of presentation makes it possible to detect the predominant wavelength more easily than with the two-dimensional transform. Measurement of wavelength could be adapted to automatic processing without great difficulty.

2.6.3. SYSTEM-OPERATING CONCEPT USING OPTICAL DATA PROCESSING

Assuming that the use of the Fourier transform procedure proves to be adequate for our purposes, the resulting system might operate in the following manner. We will consider first the problem of detecting a shoal area in open water, where the shoal area and depth have sufficient effect to produce an appreciable refraction of the waves, causing a change in direction of at least 10^{o}. Assuming the use of a satellite, imagery would be collected by means of a television system having sufficient resolution to see waves as short as 50 or 100 ft in wavelength. The television system would be continuously aimed toward the edge of the sun-glitter pattern, and imagery would be collected in such a manner as to observe the same portion of the sun-glitter pattern while the satellite traverses distances of many miles. This method of observation would assure uniformity in treatment of the wave patterns in the recording and processing operations. (The best angle of sun elevation for observing waves still remains to be determined.)

The resulting image would be placed in an optical processing system designed to scan the image using an aperture as small as practicable. It is assumed that this aperture would project an area through the system which at any instant contained perhaps ten or twenty wave crests. In addition to a recording camera, the optical processing system would include a photoelectric device capable of producing a direct measurement of the total spread and mean value of angular orientation of the primary pattern in the transform. By restricting the data collection to sea conditions which consist of regular wave patterns (straight-line, long-crested swells) with no major interferring wave trains crossing the main pattern at small intersecting angles, it would be possible to restrict the normal transform to easily predictable patterns. Any anomalous variations from the normal range of orientations would then be easy to detect and could be checked further to assure that it was produced by shoals.

We will next consider the problem of measuring the spatial extent and depth of a shoal area, the existence of which has already been detected by other means. Here again it is important to restrict the coverage to conditions in which the sun-glitter pattern is uniform over the entire area of interest and in which the incoming wave pattern is as uniform as possible. This latter requirement would be realized under conditions of calm local seas in which an incoming swell arrives from a direction that minimizes interferring patterns caused by reflection or diffraction. Ocean forecasts could be used to select periods of conditions favorable for data acquisition. If the minimum usable aperture were small enough to resolve changes in wavefront alignment over short distances, and if the automatic photoelectric recording system mentioned previously were used, it would be possible to compute and plot the orthogonal to the wavefront as a function of location on the image. If a series of continuous orthogonals could be produced in this manner, and the incoming wave velocity were known, the orthogonals could conceivably be used to compute the depth of the bottom as a function of location. The accuracy with which this can be done cannot be predicted in advance, but would have to be determined by experiment. It would be possible to carry out such an experiment by hand calculation for one or two cases to determine the feasibility of the method.

In these data-processing operations, some human monitoring would be required to preselect usable photographs and pinpoint areas of interest, but automatic processing equipment would perform the detailed analysis of the photographs.

Using a method of wavelength measurement, the data-processing operation would consist of scanning those parts of the picture which are of interest. Deep-water areas designated by the operator would be processed to provide measurements of L_o. Large areas of deep water could be scanned to provide a large sample for determining mean wavelength. Scanning of shallow areas, on the other hand, must be limited to small apertures in order to maintain fine resolution in measurement of these areas. Readout of the processor would give a mean wavelength directly. Using analog or digital processing, the wavelength at each point over shoal areas could be computed as a fraction of deep-water wavelength, and water depth of the particular point computed.

2.6.4. WAVE VELOCITY MEASUREMENTS

2.6.4.1. Moving Picture Techniques

Preliminary exploratory studies were conducted to determine the usefulness of moving pictures (or long sequences of still pictures) for measuring wave velocities, as a means of determining water depth. It appears that this technique can be used successfully, provided the pictures are taken under appropriate conditions.

It is desirable to obtain a picture sequence covering an interval of time sufficient to observe a single wave or short train of waves moving from deep water to shallow water. Obviously, the total period of time during which a small area could be kept under surveillance would be greatest if a helicopter were used as an aerial platform. If a fixed-wing aircraft is used, however, there is a definite limit for surveillance time determined by the aircraft speed and altitude, and the camera characteristics.

Assume an aircraft flying at an altitude of 20,000 ft and a speed of 250 knots (420 fps). Although the use of a moving picture camera is suggested here, even better results might be obtained with a camera designed to obtain wide-angle, high-resolution pictures at intervals of 1/2 to 1 sec. If the camera has a field of view of 74°, a single frame would cover a distance of 30,000 ft on the earth's surface. A small area would thus remain in view of the camera for a period of 72 sec, although it is not likely that the illumination conditions for observing waves would be suitable over the entire range of viewing angles. In 72 sec, a wave train of 100-ft wavelength, travelling at a speed of about 23 fps, would move a distance of 1600 ft in deep water or 1100 ft in 10-ft-deep water. These distances are sufficient in many locations to track the wave from deep to shallow water. If longer wavelengths are present, they can be tracked over even greater distances.

With a resolution of 30 lines/mm and a 70-mm frame size, the ground resolution would be about 10 ft. Image motion would not appreciably degrade this resolution, provided the exposure could be kept to 1/125 sec.

If 10-ft-deep water is to be measured by observing 100-ft waves, it would be desirable to measure wave velocity with no more than a 10% error. Even with 10-ft ground resolution, it should be possible to estimate the center of a wave crest to 10 ft. Thus, a 100-ft wave advance is needed to obtain the necessary measurement accuracy. In 10-ft-deep water, measurement accuracy requires a time interval of about 6 sec between the frames used for measurement of wave advance.

A representative system adapted to satellite application might be a television camera with a 2-in. screen having a total resolution of 5000 lines/frame and an optical system with a 12-in focal length. From an altitude of 300 nautical miles, this camera would produce a ground resolution of 60 ft and a viewing time of 13 sec. Obviously, this system would be less accurate

than the aircraft system previously described, but could be used to observe longer wavelengths. For example, this system would allow observation of a wavelength of 500 ft corresponding to a wave velocity of 50 fps travelling 650 ft, in the available viewing time.

2.6.4.2. Experiments with Motion Pictures of Waves

Wave motions were observed by means of 16-mm moving pictures taken in a flight over the eastern shoreline of Lake Michigan and from a bridge over Ford Lake. The purpose of this exploratory study was to determine the usefulness of moving pictures for measuring wave velocities and directions as a basis for determining water depth. Although the aircraft flight characteristics were not optimum for the purpose, interesting and useful results were obtained.

The pictures of the Lake Michigan shoreline show incoming waves approaching the beaches. The height and speed of the airplane were such that single waves remained in the field of view of the camera for only 3 or 4 sec. With the limited observation period available, it was not possible to follow the progress of a single wave long enough to determine its velocity with adequate accuracy. An aerial platform with a lower velocity-height ratio would therefore be advantageous for extending the period of time for observing individual waves. Individual waves could then be identified and followed for the entire period of time they were in view, indicating that it would be possible to obtain accurate measurements of wave velocity over extended distances. In many instances, an individual wave crest appears to change shape and may disappear. However, wave trains of as few as two or three wave crests will maintain their identity and can be followed by the eye.

In order to obtain usable velocity measurements, a fixed object or landmark must be present in the scene, as a reference for distance measurements, and the photographic scale must be known either from measurements of known objects in the scene itself or from a knowledge of the aircraft altitude and camera characteristics.

The pictures taken from a bridge at Ford Lake were oblique views. They were not suitable for making velocity measurements, but covered longer intervals of time than were possible with aerial photography. The movies tended to confirm the conclusions previously stated about the ability to track individual waves and wave trains for substantial periods of time.

2.7. RECOMMENDATIONS FOR FUTURE RESEARCH AND DEVELOPMENT

The work performed under the present program indicates that methods of wave analysis using aerial and space photography and optical data-processing techniques for detection and measurement of doubtful shoals are technically feasible and offer the possibility of improved performance over existing methods. Much additional theoretical and experimental research remains to be done to develop these techniques to operational status. This section outlines some directions for future research to achieve an operational capability.

2.7.1. ACQUISITION OF ADDITIONAL PHOTOGRAPHIC COVERAGE

Analysis of aerial and space photography obtained during the present project suggests some of the requirements for obtaining useful data from such coverage. By obtaining photographic coverage meeting these specifications, it should be possible to demonstrate experimentally the capabilities indicated by analysis of imagery taken under unfavorable conditions.

Pictures should be taken with both 9-in. × 9-in. aerial camera and 16- or 35-mm movie camera. Pictures of selected areas should be taken simultaneously with both types of cameras to provide comparison of results. It is preferable to take a large number of pictures of a small number of selected areas (including both beaches and open ocean) rather than single pictures at evenly spaced intervals of 10-20 sec. Pictures of beach areas should be taken from a position that produces sun glitter all the way to the shore line. (In the Lake Michigan pictures, the sun glitter was concentrated at some distance offshore, so that breakers and surf did not show up very well.)

One or more sets of pictures should be taken of areas covered by ground-truth teams. Ground truth should be collected simultaneously with the flyover. Features to observe include dominant period of breakers and character of chop, swell, and other wave components (e.g., size, orientation, and wavelength). If convenient, still pictures or movies of the offshore area should be taken. Depth measurements at points offshore should be obtained in as much detail as possible, with distances recorded offshore and alongshore from identifiable landmarks.

2.7.1.1. Aerial Camera

For each sequence of pictures, intervals between shots should be 1 to 3 sec, depending on how rapidly film can be advanced. The interval should be known to 0.1 sec or better to allow computation of speed of wave advance. An intervalometer should be used, if available. A stop watch placed at the edge of the camera frame would provide necessary accuracy.

If a 6-in. focal length camera is used (74° field of view), the frame covers a square area on the ground of 30,000 ft on a side (for 20,000-ft flight altitude). This area would stay within view for about 70 sec (at 250-knot speed), but variations in the sun-glitter pattern might limit the usable time to much less.

2.7.1.2. Moving Pictures

Color film should be used throughout the tests, since it increases the ability to discriminate detail. Pictures should be taken with the camera mounted in the aircraft for vertical photography. Camera speeds of 16 frames/sec are adequate to follow wave trains. For aircraft applications, film speed and lens opening should be chosen to permit the use of exposure as short as 1/125 sec, in order to avoid appreciable loss of resolution because of image motion. Neglecting image motion, ground resolution for a 16-mm camera at 30 1/mm from 20,000 ft would be about 25 ft.

2.7.1.3. Choice of Subject Matter

For experimental studies, ocean areas used as subjects for data collection should preferably be in the neighborhood of islands or other land masses which should appear in the imagery as convenient reference points. Areas for which there is extensive hydrographic data are desirable, although ground-truth data may be needed in addition to check some of the results. Some areas in which doubtful hydrographic data exist should also be included to provide checks on the effectiveness of the methods being developed.

Timing of coverage is as important as selection of subject areas. Past experience indicates the importance of making measurements on regular wave trains, on which there is as little interference as possible from other wave trains. Minimum interference from cloud cover is also desirable. Scheduling flights during weather conditions conducive to obtaining useful coverage should be aided by information obtained from weather- and ocean-forecasting services.

2.7.2. PROPOSED SPACE EXPERIMENT IN OCEANOGRAPHY

Experiments conducted with satellite-based, remote sensing equipment would permit further evaluation of the techniques under realistic operational conditions. In these experiments, imagery should be obtained of ocean areas known to contain shallow bottoms, e.g., areas in the Bahamas. Repeated coverage should be obtained during succeeding passes over the same test area. Preferably, coverage should be obtained under various conditions of sun elevation. It is particularly desirable to obtain coverage at times when extensive wave systems are present. Long wavelength swells arising from distant storms provide the best conditions for detecting and measuring shallow water.

Usefulness of the data would be enhanced if overlapping coverage could be obtained during a single pass. Since waves are most visible in the sun-glitter pattern, the overlapping coverage would increase the ocean area observed under conditions of best visibility. Also, if enough overlapping frames could be repeated at intervals as short as 1 sec, it might be possible to estimate wave velocities by observing the advance of individual waves.

3
MULTISPECTRAL PROCESSING TECHNIQUES FOR DEPTH MEASUREMENTS

3.1. INTRODUCTION

The shallow water features in the Caesar Creek and Pacific Reef regions off the coast of Miami, Florida, provide an ideal situation for verifying depth-measurement techniques. Caesar Creek is a ship channel which is easily recognizable in aerial imagery because of its shape and depth. The Pacific Reef has sufficient spatial variation to offer easy recognition as well as a

large variety of depths, making it useful for calibrating depth-measurement schemes. These areas are shown on the chart depicted in Fig. 11.

The availability of multispectral data for doing water-depth measurements suggests at least two techniques. One straightforward technique would be to compute spectral signatures for water of known depths in order to recognize areas of comparable depths elsewhere in the scene. Although this approach has been used successfully in recognizing surface features, the introduction of an intervening water layer—with its variable absorptance—over bottom types with variable reflectance would tend to make this approach ineffective.

The other technique, adopted for this study, overcomes this limitation; this approach utilizes a comparison of the intensities of light reflected from the ocean floor as determined by signal levels in different channels of a multispectral optical-mechanical scanner. The details of this approach are given in the following section. Because of the nature of the technique,

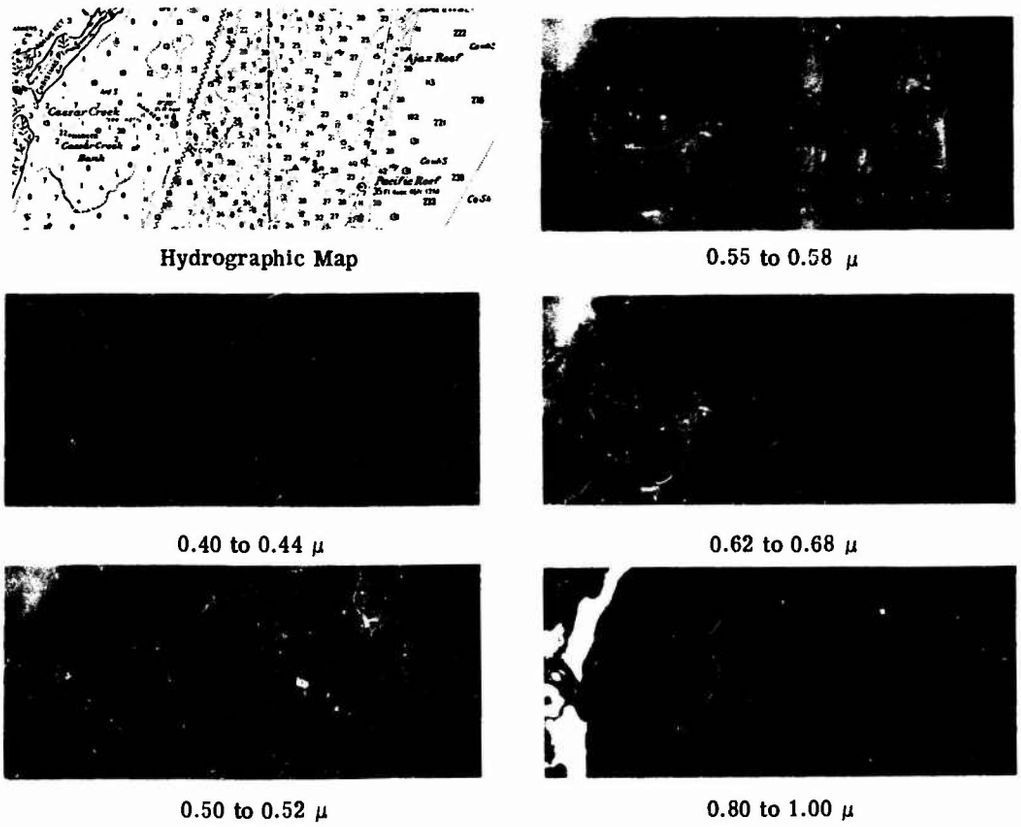

FIGURE 11. MULTISPECTRAL MAPPING OF CAESAR CREEK AND PACIFIC REEF.

variations in water absorptance and in the reflectance of the ocean floor tend to be damped out, allowing a fairly accurate depth determination over a wide area.

Because the water must be quite transparent in order to measure reflections from the ocean floor, it is only practical to use wavelengths close to 0.54 μm. The fact that the configuration of existing multispectral scanners produces only three or four usable wavelength channels imposes a slight limitation on the approach. It will be shown, however, that depths can be determined accurately in spite of this limitation. Development of a scanner with high spectral resolution from about 0.5 to 0.64 μm would serve to improve the measurements and increase the reliability of detecting shoals.

3.2. APPROACH

The electromagnetic power received by an optical system oriented toward the water consists of components of scattered sunlight (from the water and the atmosphere) and reflected sunlight (from the ocean floor and the water surface). Because the power reflected by the ocean floor must pass through an absorbing water layer, the amount reaching the system will be dependent upon the amount of absorptance which, in turn, is a function of the thickness of the water layer.

Quantitatively, this situation can be described by the following simplified equation:

$$P = \rho H e^{-(\sec\theta + \sec\phi)\alpha z} + \rho_{a/w} H + P_{scattered} \qquad (3)$$

where P = total power received

$P_{scattered}$ = power scattered (all sources)

H = solar irradiance at water surface

ρ = reflectance of ocean floor

$\rho_{a/w}$ = reflectance of air/water interface

α = absorptance of the water

z = depth of the water

θ = viewing angle (from vertical)

ϕ = solar illumination angle (from vertical)

Admittedly, this equation does not account for atmospheric absorption, differences in absorption and scattering in the light incident upon and reflected from the ocean floor, and other relatively minor effects. The inclusion of these effects, however, would greatly complicate matters without appreciably improving the accuracy of the measurements.

The equation, even in its present simple form, does not lend itself well to depth calculations because of the two terms listed last above. The elimination of these terms is accomplished by measuring P over deep water:

$$P_\infty = \lim_{z \to -\infty} P = \rho_{a/w} H + P_{scattered} \tag{4}$$

It is not quite true that these terms are the same as those in Eq. (3), since the amount of light scattered by deep water is greater than that scattered by shallow water. The difference, however, will be small, and thus it should be possible to reduce the equation to a manageable form as follows:

$$P - P_\infty = \rho H e^{-(\sec\theta + \sec\phi)\alpha z} \tag{5}$$

In practice, this is accomplished by scanning over deep water and averaging together many scan lines for each spectral channel to obtain P_∞ as a function of scan angle and wavelength. This function is then subtracted from each scan line obtained over shallow water, leaving, to first order, only the desired quantity represented by Eq. (5).

In actual applications, there are very few known quantities in Eq. (5). The power (P) is represented by a voltage (V_i) on magnetic tape, recorded from a sensor output:

$$V_i = K_i P_i \tag{6}$$

The constant, K_i, can be obtained from system calibration. In the Caesar Creek and Pacific Reef application, signals from the sensors were measured as the scanner passed over a piece of opal glass, through which sunlight was passing, at the end of each scan line. The voltage thus obtained from a given spectral channel can be represented by the following:

$$(V_s)_i = K_i (\rho_s)_i H_{\lambda i} \tag{7}$$

where s refers to the sun sensor, i refers to the channel of interest, and $(\rho_s)_i$ is the throughput of the sun sensor, determined by using standard reflectance panels on the ground. Thus, for example, if the reflectance of the scene were equal to ρ_s, the signal from the scene would have the same amplitude as the signal from the sun sensor. Since V_s and ρ_s are known, Eq. (7) can be inverted and substituted into (6) to obtain

$$V_i = \frac{(V_s)_i}{(\rho_s)_i} \frac{P_i}{H_{\lambda i}} \tag{8}$$

In turn, substitution of (8) into (5) yields

$$V_i = \frac{(V_s)_i}{(\rho_s)_i} \rho_i e^{-(\sec\theta + \sec\phi)\alpha_i z} \tag{9}$$

The expression thus obtained is in a form which can be used for depth measurements, since everything except z is either known or can be determined well enough in advance to provide reasonably accurate results.

The most troublesome quantities in Eq. (9) are ρ and α. Further manipulation of the equation can ameliorate the situation. Using two channels of data, and taking the ratio of the voltages, we obtain

$$\frac{V_i}{V_j} = \frac{(V_s)_i}{(\rho_s)_i} \frac{(\rho_s)_j}{(V_s)_j} \frac{\rho_i}{\rho_j} e^{-(\sec\theta + \sec\phi)(\alpha_i - \alpha_j)z} \tag{10}$$

Rearranging and solving for z, (10) becomes

$$z = \frac{1}{(\sec\theta + \sec\phi)(\alpha_i - \alpha_j)} \ln \frac{(V_j/\rho_j)}{(V_i/\rho_i)} \frac{(V_s/\rho_s)_i}{(V_s/\rho_s)_j} \tag{11}$$

Note that we are now concerned with <u>differences</u> in α and <u>ratios</u> of ρ.

To assess the improvement thus obtained, consider Fig. 12 which shows α for several different water conditions. Note that there are two distinct regions where $\alpha_i - \alpha_j$ is independent of water conditions:

(1) 0.55 μm to 0.64 μm

(2) wavelengths above and below (1)

Region (1) encompasses three spectral channels of The University of Michigan scanner: 0.52-0.55 μm, 0.55-0.58 μm and 0.58-0.62 μm. Because these channels have high signal-to-noise ratios and are in the region of highest water transparency, they were used in the trial runs of the depth-measuring program.

A similar consideration applies in the case of the reflectance of the ocean floor. Curves of the reflectance (see Fig. 13) of some representative wet sands show that the ratio of the reflectances of two bottom types at a given wavelength is relatively insensitive to variations in the kind of materials present.

In order to eliminate areas which were not underwater, use was made of the 0.8- to 1.0-μm channel of the multispectral scanner. For all practical purposes, water is opaque in this near infrared channel. Therefore, any signal detected in this channel (after subtracting scattered sunlight and surface reflections) would indicate an above-water feature, making depth measurement impossible. Such points were assigned a depth of zero and calculations were begun on the next point in the scene.

Computer programs were devised to (1) measure the deep-water signal, (2) subtract this measurement from the data, and (3) compute the depth according to Eq. (11). This program can be used on weighting factors applied to the combinations of spectral channels with outputs of (1) the best combination, (2) a weighted mean, and (3) a weighted deviation. The format of the out-

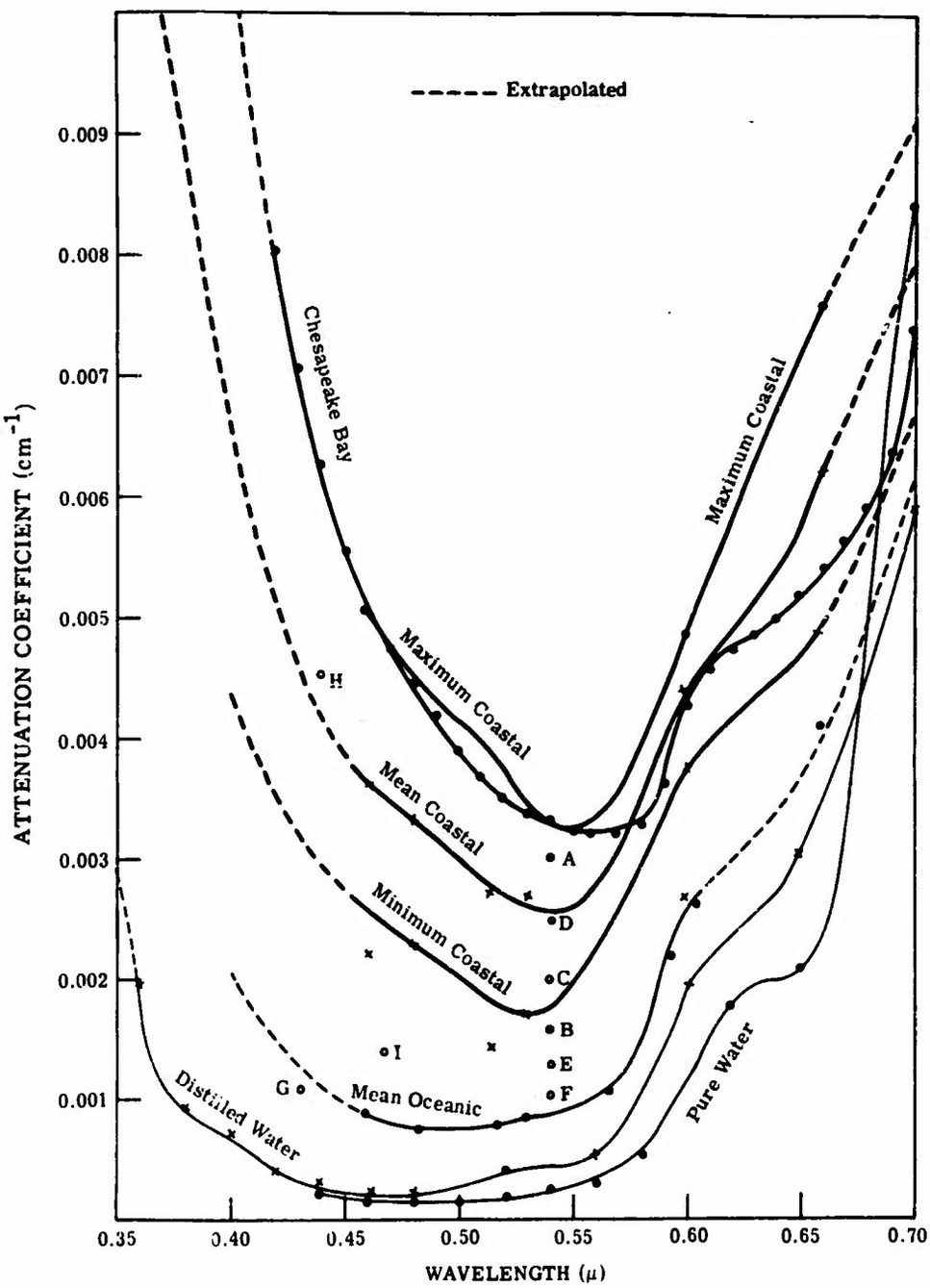

FIGURE 12. ATTENUATION COEFFICIENT VERSUS WAVELENGTH FOR PURE WATER AND SEA WATER

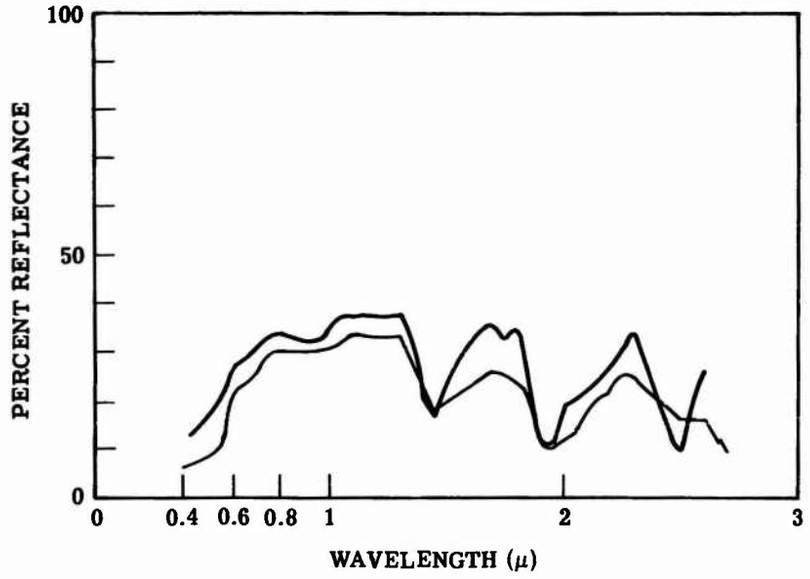

(a) Composite Plot of Reflectance from Wet, Sandy Soils (Sand, Loamy Sand)

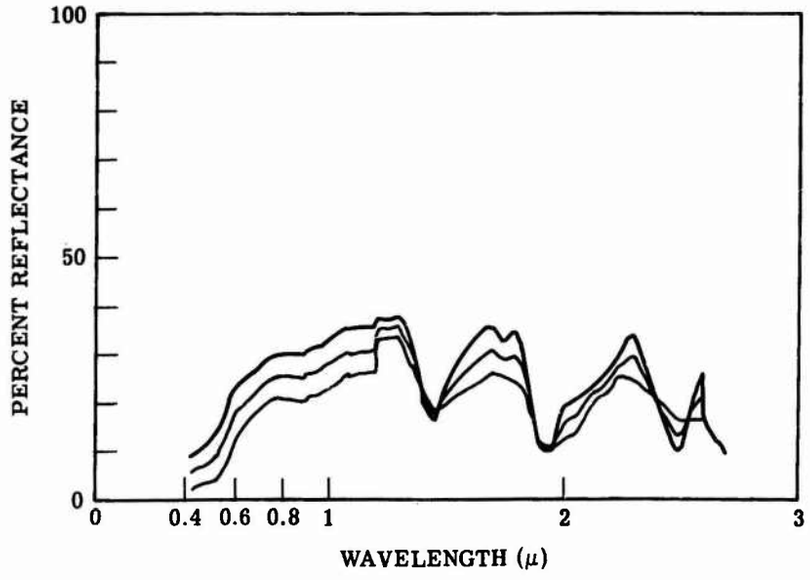

(b) Mean and Mean ± One Standard Deviation of the Reflectance from Wet, Sandy Soils (Sand, Loamy Sand)

FIGURE 13. SPECTRAL REFLECTANCE OF SANDY SOIL

puts is such that a computer map can be printed directly from them, as shown in Fig. 14. [Note: This figure was obtained from data which had been smoothed in order to diminish the effects of system noise. In effect, the spatial resolution was diminished to an effective 20 ft × 20 ft, although each point on the computer map still represents a 6.7-ft × 6.7-ft area.]

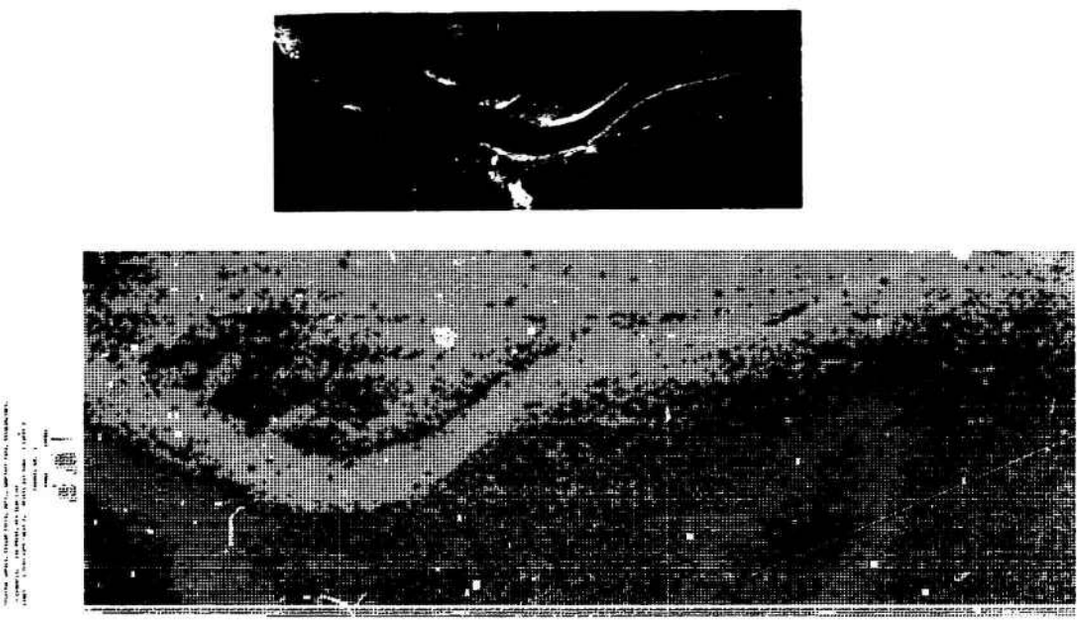

FIGURE 14. DEPTH CHART—CAESAR CREEK—OBTAINED BY DIGITAL PROCESSING OF MULTISPECTRAL SCANNING (See enlargement of Fig. 14 inserted at the end of the report.)

3.3. ANALYSIS OF RESULTS

The depth map for the Caesar Creek area was compared with the U. S. Coast and Geodetic chart of the area in Fig. 10. The deepest portion of the ship channel, according to the computer output, is 1.25 m (i.e., about 4 ft). According to the chart, the actual depth goes up to 20 ft. In the absence of onsite verification of the true depth, the following explanations are offered:

(1) The true depth is about 4 ft, because the channel has been filled in with silt.

(2) The true depth is greater than 4 ft, but the water has become clouded (e.g., by tidal action).

(3) The calculations are not as accurate as they should be.

Some hand calculations indicate that (3) is not a good explanation of this effect. Thus, we tend toward (1) or (2).

The calculations proceeded as follows. The data for spectral channel 4 (i.e., 0.52-0.55 μm) are, at the deepest point of the ship channel,

$$V_4 = 0.371$$
$$\rho_4 = \text{unknown}$$
$$(V_s)_4 = 1.60$$
$$(\rho_s)_4 = 0.14$$
$$\alpha_4 = 0.25 \text{ (mean coastal water)} m^{-1}$$
$$\theta_4 = 0.15 \text{ rad}$$
$$\phi_4 = 0.60 \text{ rad}$$

Using an inverted form of Eq. (9) and using z = 6 m, we obtain:

$$\rho_4 = V_4\left(\frac{\rho_s}{V_s}\right)_4 e^{(\sec\theta+\sec\phi)\alpha_4 z} = 0.78 \qquad (12)$$

This figure is too high. Calculations for channels 5 and 6, the other two used, yield reflectances of 1.15 and 4.57 respectively. Of course, these are physically impossible. These figures appear to be at least 8 times greater than the true values of ρ, implying that z is probably at least 3 times too large. Using z = 2 m (about 6 1/2 ft), the computed values of ρ become:

$$\rho_4 = 0.10$$
$$\rho_5 = 0.15$$
$$\rho_6 = 0.59$$

These values are certainly more realistic.

Similar values for ρ could have been obtained had we used the mean oceanic value for α (i.e., $\alpha_4 = 0.083$, $\alpha_5 = 0.115$, and $\alpha_6 = 0.25$) and the chart-obtained value of z = 6 m:

$$\rho_4 = 0.09$$
$$\rho_5 = 0.14$$
$$\rho_6 = 0.41$$

Subsequent onsite verification showed that the high signals in this area were probably the result of very turbid water occurring at the time of high tide.

3.4. VARIABILITY IN THE DATA

There are at least three sources of variability of the data put out by the depth-measurement analysis: (1) system noise, including the analog-to-digital quantization of signal levels; (2) uncertainties and/or variations in the turbidity of the water and in the reflectance of the ocean floor; and (3) uncertainties and/or variations in the deep-water signal levels, including sun glint and wave phenomena. In addition to these factors, the equations which have been programmed are greatly simplified.

In the face of these observations, it is interesting to note that the measurements which have been obtained are in agreement with the charts of the area. Onsite inspections should remove uncertainties which still remain.

Aside from considerations of the accuracy of the results, there is the question of verification of the results when using different combinations of spectral channels. Several computer maps of the same area shown in Fig. 13 were made, comparing the results using different combinations of data channels 4, 5, and 6. Each combination was weighted by a normalized function proportional to the difference in absorptances of the pair of spectral channels being used. It was verified that the large difference in absorptances provides greater confidence in the calculations.

In future work on this problem, it is hoped that onsite depth measurements and/or the inclusion of a laser depth-measuring device will provide calibration of the technique.

4
LASER-RANGING TECHNIQUES FOR IDENTIFYING SHALLOW WATER FEATURES

An earlier study conducted under this program (see Ref. 1) concluded that water depth could be determined directly by use of an optical laser system which would measure the time difference between the laser-beam reflection from the water surface and the reflection from the bottom. Because of some ambiguities and errors in the discussion of this technique in Ref. [1],the discussion which follows is intended to supplement and update the previous annual report.

The performance of a laser-ranging system in depth measurements is dependent upon many variables, including spectral characteristics, geometric factors, and system design parameters. Further constraints are effected by size, weight, and power limitations imposed by the platform (i.e., the aircraft or satellite), as well as by the altitude and velocity of the platform.

Referring to the earlier study, the maximum depth of penetration of the laser beam in water can be expressed as follows:

$$r = \frac{1}{2\alpha} \ln \left\{ \underbrace{\rho_b \tau_a^2 (1 - \rho_w)^2 \left[\frac{\cos \theta}{\pi (h + r)^2} \right]}_{\text{Term 1}} \underbrace{\left[\frac{P_t \tau_t \tau_r A_r}{(SNR) \left(\frac{2ek^2 \Delta f P_r}{S_c} \right)^{1/2}} \right]}_{\text{Term 2}} \right\} \qquad \text{Term 3} \qquad (13)$$

Term 1 is the spectrally dependent term; term 2 represents the geometric factors such as altitude and angle of incidence; and term 3 encompasses the laser equipment parameters. The

derivation of Eq. (13) is presented in the appendix to Ref. [1]. The definition of symbols for this and the following equations are given below:

r = depth of water
α = absorption coefficient of water
P_t = transmitter power
τ_t = transmittance of transmitter optics
τ_r = transmittance of receiver optics
τ_a = transmittance of air
ρ_b = reflectance of ocean bottom
$1 - \rho_w$ = air/water transmittance
A_r = area of receiver collector
S_c = photomultiplier cathode sensitivity (A/W)
θ = angle between transmitter axis and water surface normal
h = height of aircraft or spacecraft
SNR = signal-to-noise ratio
e = electronic charge
k = secondary emission factor
Δf = electrical bandwidth
P_r = received signal power

The depth equation (13) is simplified in that all noise sources to the photomultiplier receiver are ignored except the shot noise caused by P_r, the signal power received at the detector. Since the other sources of noise are generally from 4 to 44 orders of magnitude less than P_r, their contribution is negligible. The signal power is given by

$$P_r = \underbrace{\rho_b \tau_a^2 (1 - \rho_w)^2 e^{-2\alpha r}}_{\text{Term 1}} \underbrace{\left[\frac{\cos\theta}{\pi(h + r)^2}\right]}_{\text{Term 2}} \underbrace{P_t \tau_t \tau_r A_r}_{\text{Term 3}} \tag{14}$$

As before, term 1 is the spectrally dependent term; term 2 is geometrically dependent; and term 3 covers system parameters.

Substituting P_r into the depth equation (13), it can be seen that the required magnitude of P_r is dependent upon the signal-to-noise ratio (SNR) and photomultiplier cathode radiant sensitivity (S_c) as follows:

$$P_r = (SNR)^2 \left(\frac{2ek^2 \Delta f}{S_c}\right) \tag{15}$$

Using this result, P_r can be eliminated from the range equation, leaving

$$r = \frac{1}{2\alpha} \ln\left\{\rho_b \tau_a^2 (1 - \rho_w)^2 \left[\frac{\cos\vartheta}{\pi(h + r)^2}\right]\left[\frac{P_t \tau_t \tau_r A_r}{(SNR)^2\left(\frac{2ek^2\Delta f}{S_c}\right)}\right]\right\} \qquad (16)$$

Inversion of the range equation (16) shows that the peak power required to penetrate to a given depth of water is proportional to $e^{2\alpha r}$, illustrating that the power required by the transmitter increases rapidly with small increases in α. For this reason, it is mandatory that the laser output fall in the 0.51-μm to 0.56-μm portion of the spectrum, where α is relatively small. From physical characteristics data (see Ref. 1, p. 52), it is seen that high-powered lasers ($P_t \geq 10^6$ W) exist for 5 wavelengths in the 0.3-μm to 0.7-μm spectrum, with 2 of these in the low α region. Table 2 lists these wavelengths, the corresponding attenuation coefficients for mean coastal waters, and the attenuation ($e^{2\alpha r}$) for depths of 10 m and 1 m.

TABLE 2. WAVELENGTHS AND CORRESPONDING COEFFICIENTS FOR MEAN COASTAL WATERS, AND THE ATTENUATION FOR DEPTHS OF 10 m AND 1 m

Wavelength	Attenuation Coefficient	Attenuation For 10- Depth	Attenuation For 1-m Depth
0.3371	1.45	3.9×10^{12}	18.2
0.3472	1.24	5.9×10^{10}	11.9
0.5300	0.252	154	1.66
0.5510	0.264	196	1.70
0.6943	0.785	6.6×10^6	4.81

It is quite evident from the table that the attenuation outside the 0.51-μm to 0.56-μm region is excessive for most of the depths of interest. Table 3 presents other parameters of interest for the same 5 lasers.

The choice of a laser with a high peak power (P_t) at the wavelength of the minimum attenuation coefficient for coastal waters appears to afford the greatest potential for depth penetration to identify shallow water features. Table 4 gives characteristics for lasers operating in the

TABLE 3. ADDITIONAL PARAMETERS FOR SAME FIVE LASERS

	Atmospheric Transmission			
Wavelength	0.5 km	200 Nautical Miles	Coastal Seawater Reflectance	Ocean Floor Reflectance
0.3371	0.843	0.342		
0.3472	0.856	0.380		
0.5300	0.933	0.715	0.0612	0.04-0.24
0.5510	0.938	0.758	0.0545	0.06-0.36
0.6943	0.960	0.798		

TABLE 4. CHARACTERISTICS FOR LASERS OPERATING IN THE 0.3-μm TO 0.7-μm REGION

Wavelength (μm)	Type	Material	Output (j)	Peak Power (W)	Pulse Width (nsec)	PRF (Hz)	Efficiency (%)
0.3371	Gas	N_2 in air	0.1	10^6	4	100	1.0
0.3472*	Solid State	$Cr^{3+}:A\ell_2O_3$	75	100×10^6	10	100	0.01
0.5300*	Solid State	Nd^{3+}:Glass	300	560×10^6	10		1.0
0.5300*	Solid State	Nd^{3+}:YAG	30	56×10^6	10	100	1.0
0.5510 / 0.5950	Liquid Dye	Rodamine 6G in CH_3HO	150	2×10^6	5	1500	0.036
0.6943	Solid State	$Cr^{3+}:A\ell_2O_3$	1500		10	100	0.1

*Second Harmonic. Operating temperature = 300°K for all three wavelengths. Beamwidth = 1 mrad for all except: Nd^{3+}:Glass (7.5 mrad)
$Cr^{3+}:A\ell_2O_3$ (2 mrad at 0.6943 μm)

0.3-μm to 0.7-μm region. This listing of Q-switched lasers has standardized the outputs to 10-nsec (or less) pulses at a pulse-rate-frequency (PRF) of 100 Hz. Since the output power is a constant percentage (70% and up) of the rated average output power, higher PRF's and narrower pulse widths must be traded off at the expense of lower peak powers and higher processing bandwidth requirements.

The most powerful laser listed in Table 4 is the second harmonic of the 1.06-μm Nd^{3+}:Glass laser. A large laser, its rod is 94-cm long with a 3.8-cm outside diameter and a 3-cm core diameter. A closed-cycle liquid cooling system is required. Optical pumping is provided by four 1-m flashtubes with a required total input power of 180 W.

Electronic processing of the laser data is complicated because of the narrow pulses involved. For example, a 5-nsec pulse width requires high signal-to-noise ratios and 200-mHz bandwidths in the video amplifiers and preamplifier. The range resolution R_n in water for such a system is given by

$$R_r = \frac{CT}{n_w}$$

where C = velocity of light in vacuo (2.99793×10^8 m/sec)
T = pulse width (sec)
n_w = index of water refraction (1.33338).

Thus, the range resolution for a 5-nsec pulse-width is 1.12 m. Range resolution can be improved an order of magnitude by using a 2-gate system which tracks the received signals from the water surface and ocean floor, but it is difficult to implement with a single pulse (i.e., no integration). The fine resolution described above will be degraded somewhat because of the scattering of the beam in the water and (for the satellite case) the curvature of the earth, both of which cause stretching of the received signal pulses.

The peak power which will be used depends indirectly upon the desired data rate. If it is assumed that a data point is desired for every meter of flight line traversed, an aircraft flying at 120 knots will require a PRF of 60 Hz and a satellite orbiting at an altitude of 200 nautical miles will require a PRF of 7500 Hz. Using a pulse-width of 10 nsec, the peak power of the highest power Nd^{3+}:Glass laser will be 5×10^8 W for aircraft and 4×10^6 W for spacecraft.

The required power input to the Nd^{3+}:Glass laser is 180 W, which can be supplied in an aircraft but which might pose problems in a satellite. Since almost all (99.76%) of this input power has to be dissipated as heat with liquid coolant and heat exchangers, the satellite will be further burdened by the size and weight of the cooling system for the laser. It is probable that in a satellite laser output, peak power may have to be sacrificed in order to obtain acceptable weights for prime power and cooling systems.

4.1. OPERATIONAL CONSIDERATIONS

Data processing, whether by automatic equipment or human operators, requires that the signal be greater than the system noise. Human operators require less signal-to-noise ratio (SNR) than machine processors. Since the data rates are 60 points/sec for aircraft and 7500 points/sec for a satellite, human operators will be unable to handle the results. Thus, automatic data processing will be required and higher SNR will be necessary.

Digital communications and pulsed radar theory show that SNR = 11.1 is required for a probability of error equal to 0.1; further reduction of the probability of error to 0.01 (1%) requires SNR = 20. All calculations which follow are based on the higher SNR, yielding a detection probability of 99%.

The accuracy of the results will be affected by refraction of the laser beam by the water. If the beam strikes the water at an angle, it will be refracted toward the normal. The angle at which the beam strikes the water will in turn be affected by the presence of waves. The average slope angle of ocean waves usually varies from about 3 min to 6°, although the shallow depths of coastal waters can increase this to 19°. With such high incidence angles, the laser beam will be refracted away from the normal and the measured depth will be too large, indicating deeper-than-actual water, the opposite indication from what is needed for identifying hazardous underwater features.

Much of the problem caused by surface wave effects can be eliminated by scanning. To maintain the same spatial resolution, therefore, the data rate will have to be increased. The increased data rate will result in decreased peak power of the laser transmitter because of the required increase in the PRF.

4.2. PERFORMANCE CALCULATIONS

A computerized tradeoff study of laser depth-ranging systems was presented in Ref. [1]. Following publication of the study, it was discovered that errors in the computer outputs changed the results of the study. Rather than completely redoing the tradeoff studies, it was decided that some typical parameters would be used to make the calculations in order to give an idea of what is practical at present. Table 5 lists those typical parameters for a profiling system carried by an aircraft at a 0.5-km altitude and in a satellite orbiting at a 200-nautical-mile (370-km) altitude. In both cases, a 0.5330 μm Nd^{3+}:Glass laser was used, with a data patch spacing of 1 m. An RCA 7029 photomultiplier (S-17 spectral surface) is used in both receivers. On the basis of the data listed in Table 6, the values of αr and of r (for mean coastal waters) were calculated and are given in Table 6.

TABLE 5. LASER DEPTH-RANGING SYSTEM PARAMETERS AND OPERATIONAL CONDITIONS

Operational Conditions	Aircraft	Satellite
Altitude (km)	0.5	370
Ground Speed (m/sec)	62	7475
Illuminated Patch Diameter (m)	0.05	1.85
Physical Environment		
Atmospheric Transmittance (τ_a)		
Clear Day	0.933	0.715
Hazy Day (Sea Level α = 1 km^{-1})	0.617	0.279
Air/Water Transmittance (1 - ρ_w)	0.945	0.945
Ocean Floor Reflectance (ρ_b)	0.10	0.10
Laser System Parameters		
Transmitter: Type	1-Stage Oscillator	1-Stage Oscillator
Peak Power (W)	5×10^8	8×10^6
Pulse Width (nsec)	10	10
Pulse-Repetition-Frequency (Hz)	60	7500
Power Input (W)	180	360
Aperture Diameter (cm)	20	1900
Beam (mrad)	2.1	0.005
Transmittance of Optics	0.97	0.97
Receiver: Type	Pseudo-Cassegrainian	Pseudo-Cassegrainian
Aperture Area (m^2)	1.0	1.0
Transmittance of Optics	0.450	0.450
Electronic Bandpass	100 mHz	100 mHz
SNR	20	20

As indicated by the figures in Table 6, significant depth penetration from satellite altitudes can be obtained only at the expense of reliability of detection. This would indicate that the data rate (PRF) must be reduced and/or the input power increased in order to regain reliability at satellite altitudes. The implications of such modifications have been discussed previously.

TABLE 6. VALUES OF αr AND OF r
(FOR MEAN COASTAL WATERS)

Platform	αr	r(m)	Detection Probability
Aircraft			
Clear Day	9.5	38	0.99
Hazy Day	9.1	36	0.99
Spacecraft			
Clear Day	0.37	1.5	0.99
	1.06	4.2	0.82*
Hazy Day	0.10	0.4	0.82*

*SNR = 10

REFERENCES

1. F. C. Polcyn and R. A. Rollin, Remote Sensing Techniques for the Location and Measurement of Shallow-Water Features, Report No. 8973-10-P, Willow Run Laboratories of the Institute of Science and Technology, The University of Michigan, Ann Arbor, January 1969.
2. P. L. Jackson, "Diffractive Processing of Geophysical Data," Appl. Opt., Vol. 4, No. 4, April 1965, pp. 419-427.
3. Graphical Construction of Wave Refraction Diagrams, U. S. Naval Oceanographic Office, H. O. Pub. No. 605, 1964.
4. P. L. Jackson, "Sectional Correlograms and Convolutions by a Simple Optical Method," Geophysics, Vol. 33, No. 5, October 1968.
5. Vincent Noble, Ocean Swell Measurements from Satellite Photographs, Remote Sensing of Environment, Vol. 1, No. 3, Summer 1970, pp. 151-154.

FIGURE 14. (Repeated) DEPTH CHART—CA
PROCESSING OF MULTISI

DEPTH IN METERS

RANGE		SYMBOL
0	0	
0	.3140	X
.3140	.6260	0
.6260	.9390	*
.9390	1.2520	=
1.2520	1.5440	-
1.5440	10.0000	

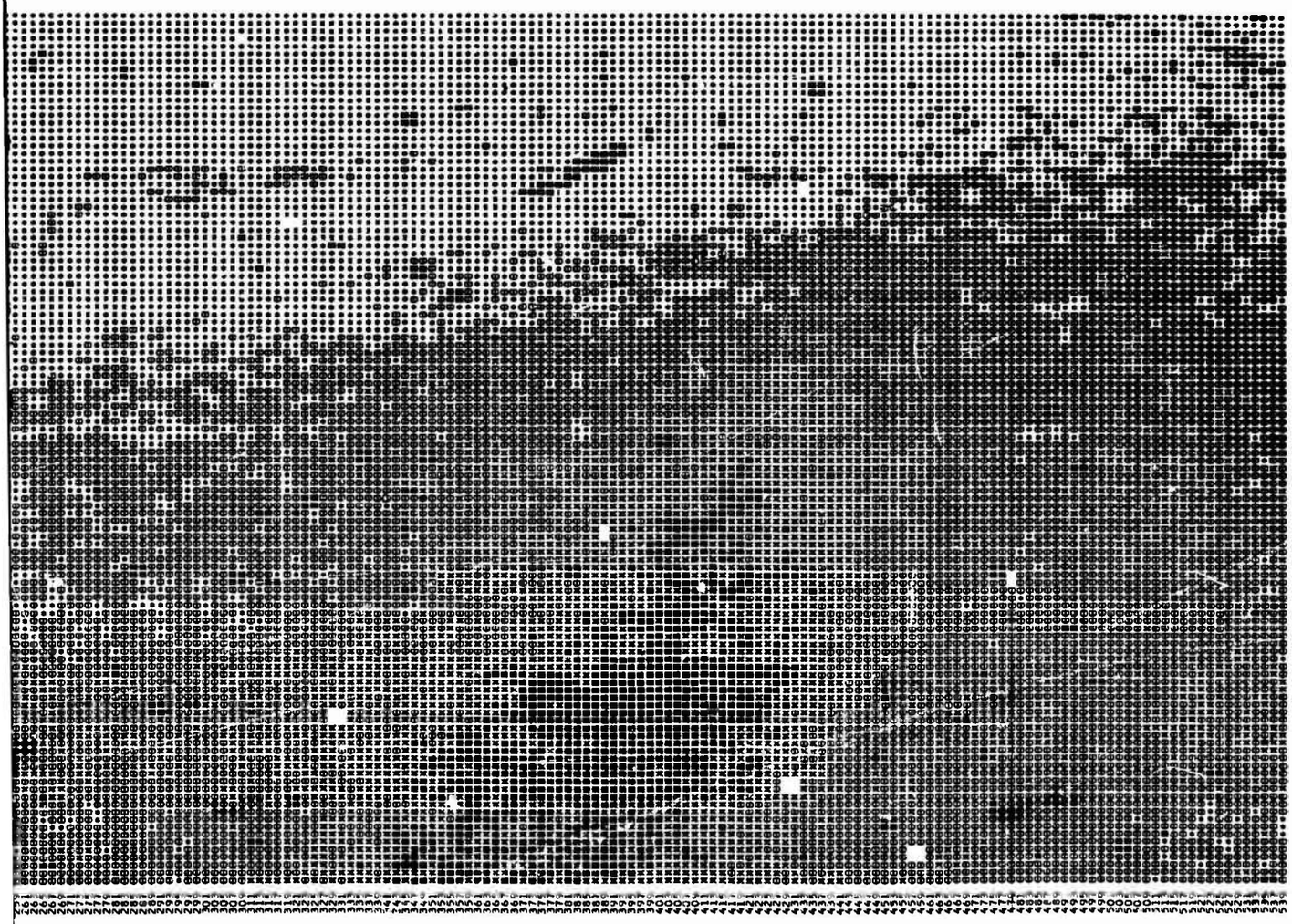

CAESAR CREEK—OBTAINED BY DIGITAL
TISPECTRAL SCANNING

B